Electron-Induced Cascade Showers in Copper, Tin, and Lead*

CAROL JO CRANNELL†
High Energy Physics Laboratory, Stanford University, Stanford, California

(Received 1 May 1967)

Electromagnetic cascade showers induced by 900-MeV electrons have been studied in copper, tin, and lead targets. A small, parallel incident beam with negligible background contamination was employed to achieve good resolution and undistorted development of the shower. The three-dimensional spatial distribution of energy deposition was measured with a CsI(Tl) detector placed at various positions in a small hole in an otherwise solid block of material. Measurements were extended to radii of 7 Molière lengths and depths of 30 or more radiation lengths. Additional data for showers induced by 200-MeV electrons incident on lead are also presented. The results of this experiment are compared with the results of previous experiments and with the predictions of recent Monte-Carlo calculations. The measured longitudinal distribution of energy is in good agreement with theoretical predictions, while the radial distributions show an unpredicted dependence on the atomic number of the target material.

I. INTRODUCTION

COSMIC rays produced the first experimentally observed electromagnetic cascade showers. The shower events seen in cloud chambers are characterized by a single initial track, indicating the passage of an ionizing particle, successively branching into more and more tracks until the energy supplied by the initiating particle has been so partitioned that none of the remnants has sufficient energy to ionize the chamber medium. The principal phenomena responsible for the development of a shower and the analytical descriptions of the longitudinal development of a shower have been discussed by Rossi.[1] Wilson[2] calculated the energy deposition as a function of depth, called the transition curve, using a Monte-Carlo technique. Improved Monte-Carlo calculations have been performed by Messel *et al.*,[3] Zerby and Moran,[4] Nagel,[5] and Völkel[6] for the three-dimensional development of the shower. The program developed by Nagel and used by Nagel and Völkel considered lower-energy partitioning of the shower than any of the previous work.

Experimentally, the behavior of the showers has been investigated by a variety of techniques. The two characteristics of greatest interest are the energy spectra of particles in the shower and the energy deposition as a function of position in the shower. Kantz and Hofstadter[7,8] obtained the first measurements of the radial as well as the longitudinal deposition of energy in electron-induced showers. When the present experiment was begun, there was interest in obtaining experimental data at higher incident energies than previously investigated. If the results for incident-electron energies near the limit of then existing accelerators confirmed the predictions of Monte-Carlo calculations, then the Monte-Carlo predictions for even higher incident energies could be used with more confidence.

In this experiment the technique developed by Kantz and Hofstadter is used to obtain information on the deposition of energy, both radially and longitudinally,[9] for a shower initiated by a beam of 900-MeV (± 4 MeV) electrons. Whenever it was possible, the equipment was improved and the data acquisition and reduction were automated. Improvements in the Stanford Mark III linear accelerator and in the beam transport system have made it possible to obtain a well-collimated beam of 900-MeV electrons without the use of a collimator after the sweeping magnet. The results obtained for the longitudinal development compare favorably with the recent experiment of Nelson *et al.*,[10] as well as with the Monte-Carlo calculations of Zerby and Moran, and Nagel. Similar comparisons of the lateral development show significant differences. Some additional data for 200-MeV electron-induced showers in lead were obtained to compare with the results of Murata[11] which

* Work supported in part by the U. S. Office of Naval Research [Contract Nonr 225 (67)] and in part by the National Science Foundation, Grant NSF GP-948.

† Present address: Physics Department, The Catholic University of America, Washington, D.C.

[1] B. Rossi, *High-Energy Particles* (Prentice-Hall, Inc., Englewood Cliffs, New Jersey, 1952).

[2] R. R. Wilson, Phys. Rev. **86**, 261 (1952). For corrections to this paper see H. Thom, *ibid.* **136**, B447 (1964).

[3] H. Messel, A. D. Smirnov, A. A. Varfolomeev, D. F. Crawford, and J. C. Butcher, Nucl. Phys. **39**, 1 (1962); D. F. Crawford and H. Messel, Phys. Rev. **128**, 2352 (1962); Nucl. Phys. **61**, 145 (1965).

[4] C. D. Zerby and H. S. Moran, Oak Ridge National Laboratory Reports Nos. ORNL-3329, 1962 (unpublished); ORNL-TM-422, 1962 (unpublished); J. Appl. Phys. **34**, 2445 (1963). Also a calculation of 950-MeV electron-induced showers in copper was carried out by C. D. Zerby and H. S. Moran for the Stanford Linear Accelerator Center and made available to this author by W. R. Nelson.

[5] H. Nagel, Z. Physik **186**, 319 (1965).

[6] U. Völkel, Deutsches Elektronen-Synchrotron 65/6, 1965 (unpublished).

[7] A. Kantz, Ph.D. thesis, Stanford University, 1954 (unpublished); Stanford University High Energy Physics Laboratory Report No. 17, 1954 (unpublished).

[8] A. Kantz and R. Hofstadter, Phys. Rev. **89**, 607 (1953); Nucleonics **12**, 36 (1954).

[9] The radial and longitudinal distributions of energy deposition for 900-MeV electron-induced showers in copper, tin, and lead and for 200-MeV electron-induced showers in lead are presented for this experiment in the form of energy-block diagrams similar to those devised by Kantz and Hofstadter. These tables are available from the High Energy Physics Laboratory, Stanford University, Stanford, California as HEPL Technical Note Number 67-4 (unpublished).

[10] W. R. Nelson, T. M. Jenkins, R. C. McCall, and J. K. Cobb, Phys. Rev. **149**, 201 (1966).

[11] Y. Murata, J. Phys. Soc. Japan **20**, 209 (1965).

TABLE I. Numerical parameters associated with the target elements.

Target element	Z	A	Dimensions of target (cm^3)	Density ($g\ cm^{-3}$)	χ_0[a] ($g\ cm^{-2}$)	ϵ_0[b] (MeV)
Copper	29	63.6	61×61×61	8.82	13.1	18.8
Tin	50	119	30.5×30.5×46	7.3	8.93	11.4
Lead	82	207.2	30.5×30.5×46	11.3	6.5	7.4

[a] Calculated using Eq. 5.2(1) of Rossi (Ref. 1). and found to be in good agreement with the corresponding values given by O. I. Dovzhenko and A. A. Pomanskii, Zh. Eksperim. i Teor. Fiz. **45**, 268 (1963) [English transl.: Soviet Phys.—JETP **18**, 187 (1964)].

[b] The critical energies for copper and lead were tabulated by Dovzhenko and Pomanskii and the critical energy for tin was calculated using the expression presented in their article.

show small differences from the results of Kantz and Hofstadter.

II. EXPERIMENTAL TECHNIQUES

A. Equipment

The materials used as targets for this experiment are square plates of copper, tin, or lead. These were pressed together with a hydraulic jack to simulate a solid block of material with the plane of each plate perpendicular to the beam axis. The effective densities of each material were measured in this configuration and were found to agree with the nominal densities of the solid material to within better than 1%. The dimensions, densities, and other numerical parameters associated with the three targets are given in Table I, and a drawing of the apparatus is shown in Fig. 1. Each plate was oriented so that a corner rested in the trough of the support frame. This enabled the experimenter to reposition the plates accurately and easily.

The detector is a thallium-activated cesium-iodide crystal [CsI(Tl)] which is observed by an EMI 6094B photomultiplier tube through either a polished aluminum tube (air light pipe) or a lucite light pipe surrounded by a polished aluminum tube. The photomultiplier is protected from the background radiation in the target area by a 5-cm-thick lead chimney. The chimney is bolted to a 1.27-cm-thick plate of the target material in which a 0.95-cm hole, called a probe well, has been drilled. The hole into which the detector is inserted is positioned along the diagonal axis of the plate, and extends from 5 cm below beam axis to the corner of the plate. The detector-photomultiplier assembly, called the probe, is movable in steps of 0.025 cm so that the detector can be positioned accurately anywhere along the hole. (See Fig. 1.) The probe plate, with the chimney and probe, can be moved to any depth in the target to obtain information on the longitudinal development of the shower.

The primary monitor of the incident-electron beam intensity is an ion chamber which is bolted to the exit end of the beam pipe. A secondary monitor consisting of a photomultiplier-detector assembly similar to the probe assembly was also used. It was inserted in a second drilled plate, called the monitor plate, always situated more than 4 radiation lengths behind the probe plate.

B. Data-Acquisition Procedure

Before a radial distribution curve was measured, a procedure was followed to ensure that the detector would pass through the center of the core of the shower when the radial data were measured. The probe was moved up and down until the detector was approximately on the beam axis; then the beam was steered left and right until the maximum signal from the probe was obtained. This centering could be achieved to ± 0.03 cm.

The signals from the probe and the monitor were amplified, recorded on a dual-pen strip chart recorder, and transmitted by the experimenter to an experimental IBM data-acquisition system via a teletype.[12] The probe position along the radius from the beam axis and the gain settings on the amplifiers were displayed to the experimenter on Nixie lights and were also read directly by the data acquisition system. The IBM system typed out the probe signal-to-beam intensity ratio and also plotted the ratio versus radial position as the data were being acquired.

Between the times when the experimental points were recorded, the beam was turned off and the residual current from the photomultiplier(s) was canceled manually by the zero adjustments on the amplifier and on the recorder. Additional background was caused by Čerenkov radiation in the light pipe and radiation from the target area reaching the probe photomultiplier. By removing the CsI(Tl) crystal from the probe assembly and measuring the radial distribution of the remaining signal, the size of this effect could be determined. Although negligible over the major portion of the shower, this background was measured or calculated by interpolation for each radial distribution curve. It was found to be less than 0.1% of the signal near the shower axis and less than 10% near the edge of the radial distribution. Uncertainty in the measurement of the background caused at worst a 3% error in any portion of any radial curve.

[12] P. Friedl, C. Sederholm, W. Dye, H. Crannell, and M. R. Yearian, J. Computational Phys. 1, 305 (1967).

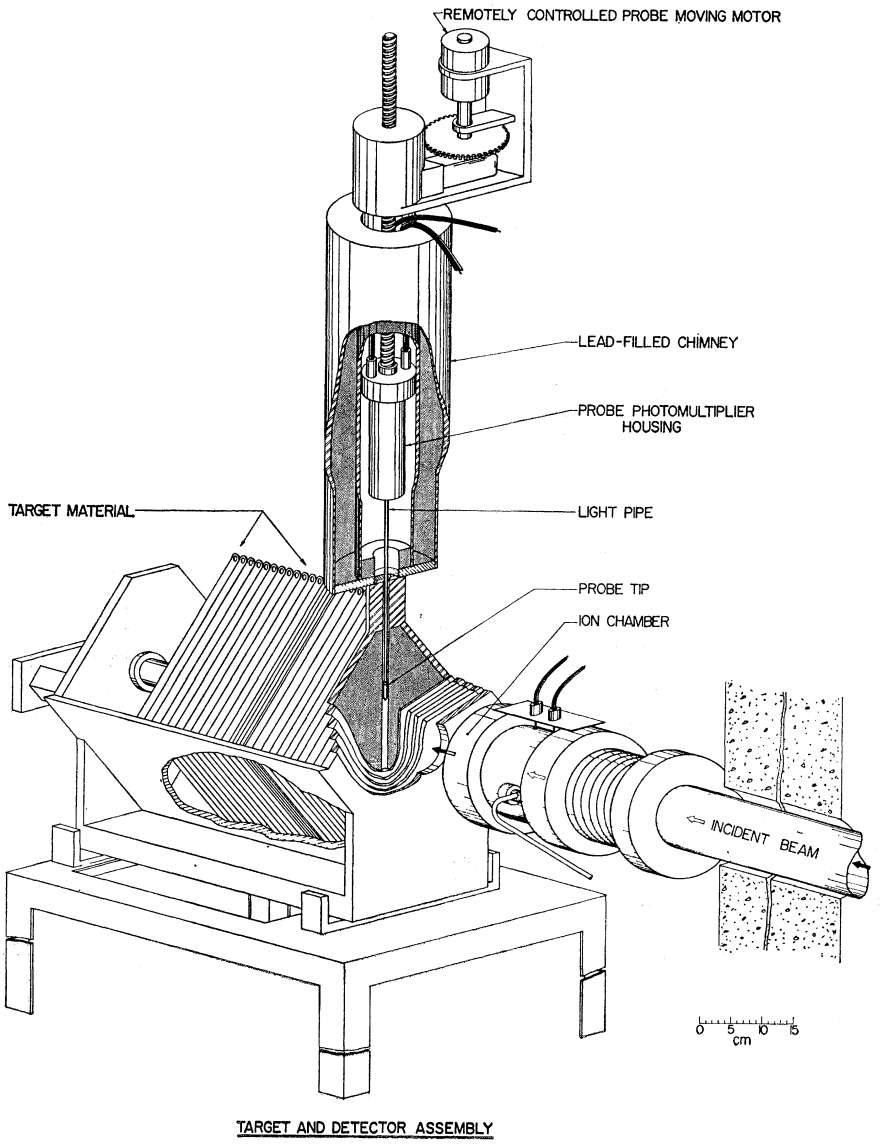

FIG. 1. The target and detector assembly is shown with the beam-monitoring ion chamber aligned with the incident beam. The plates shown in the target frame are the same size as the lead and tin plates used in this experiment.

C. Experimental Checks

To check the linearity of the response of the ion chamber, the signal from the ion chamber was compared with the signal from the secondary monitor over a range of beam intensities for which the secondary monitor was known to be linear. In this manner the ion chamber was found to be linear to within 3% over a useful range of two decades. The lower limit is determined by the sensitivity of the amplifier and the upper limit by the space-charge saturation of the chamber. Care was taken never to operate the chamber outside this range of beam intensities. Similarly, saturation curves for each photomultiplier used in this experiment were measured for a variety of high voltages. The tubes were operated well within their regions of linearity, with care being taken to avoid fatigue effects by never permitting the output current to exceed the saturation level.

While the preliminary data were being taken, it was found that the efficiency of the secondary monitor varied as the probe and probe plate assembly were moved to different depths in the shower. The total amount of material in front of the monitor plate was kept constant and the probe plate was moved from 6 to 20 radiation lengths forward of the monitor plate. The maximum change in monitor efficiency (ratio of the signal from the secondary monitor to the signal from the ion chamber) was found to be approximately 25%. It was then determined that the monitor efficiency also varied as the detector moved in the radial direction across beam axis. The detector was mounted on a brass plug (similar to those shown in Fig. 2) which was held in the aluminum tube with a rubber O-ring seal. When

the monitor efficiency, as a function of radial position of the probe, was studied in detail, a precise outline of the brass probe tip emerged with a 12% maximum variation of the efficiency. To reduce the effect due to the probe tip, the detector was mounted on a short, hollow aluminum plug. The passage of this probe tip through the core of the shower had negligible effect on the secondary monitor; however, the radial distribution curves measured with the hollow aluminum probe tips were significantly broader than the distributions measured with the brass plugs. At a longitudinal depth of 5.5 radiation lengths in tin and a radial distance of 12 radiation lengths from the beam axis, the measured energy deposition was 100% larger with the aluminum plugs than with the brass plugs.

A set of plugs was then made with lengths from 0.1 to 4 radiation lengths. To study the effect of the amount of material between the shower axis and the crystal, the same radial distribution curve was measured with each of the plugs. The curve was found not to vary for all probe tips longer than 2 radiation lengths, but the curve was found to be between 10 and 100% higher for the probe tips less than 2 radiation lengths long. Since in a solid material there would be no probe well, it is reasonable that the measurements made with the longer probe tips give the best representation of energy deposited in unperturbed shower development. Therefore, for all the data measured in this experiment, probe tips greater than 2 radiation lengths long were used.

To eliminate the effect which was due to the probe tip and the probe well on the efficiency of the secondary monitor, the primary monitor was used in the measurement of radial distribution curves, except when the probe tip was far from the shower axis. The energy deposition varied over a wide range (as much as 10^8) in some of the radical distribution curves. The signal from the probe occasionally became too small to measure without raising the beam current to a level (greater than 10^7 electrons per pulse) that saturated the ion chamber. By adjusting the depth that the monitor is inserted into the blocks, the lower range of the secondary monitor can be made to overlap the upper linear range of the ion chamber, thus extending the range over which the beam intensities can be monitored. Before the beam intensity was increased, the secondary monitor was calibrated against the ion chamber. It was calibrated again when the distribution had been completed and before the probe assembly was moved to another depth.

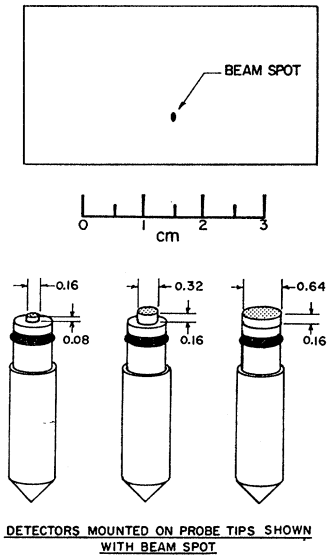

FIG. 2. The image of the incident beam is shown with the three different-size CsI(Tl) detectors. The image was formed by passing the beam through a thin plate of glass until a saturated area of color centers was developed. The vertical extent of the beam is seen to be larger than its horizontal extent.

To obtain an accurate determination of the energy deposited as a function of position in the shower, the beam of electrons must be well collimated and incident normally on the target. It is also important that the detector should be small with respect to the distance in which the rate of energy deposition changes significantly. The size and shape of the incident beam were measured by exposing a glass slide until the center of the image was thoroughly saturated. A typical beam spot image obtained in this way is pictured in Fig. 2. The angular spread of the beam was measured by removing all the plates from the target frame and measuring the radial distribution of the beam at the front and the back of the frame. The spread was less than 0.2° in 60 cm.

Three crystals of different sizes were prepared for three overlapping regions of the shower. The crystals were as small as could be used to obtain a reasonable signal-to-noise ratio. The sizes and the corresponding regions of investigation are: 0.08 cm high by 0.16-cm diam for the early part of the shower, 0.16 cm high by 0.32-cm diam over shower maximum, and 0.16 cm high by 0.64-cm diam beyond shower maximum to the final measured depth. The smallest crystal is small with respect to the dimensions of the incident beam (see Fig. 2), but not small with respect to the distance in which the distribution was observed to decrease by a factor of e (as small as 0.05 cm in the early part of the shower). However, the effect of the finite crystal size is calculated to be less than a 10% increase or decrease in even the most sharply peaked radial distributions. For the depths at which the other two crystals were used, calculations indicated the resolution would have negligible effect. The results were checked experimentally by repeating the radial distribution curve at the depth where the crystal size was changed. This technique confirmed the predictions of the calculations, and provided a measurement of the factor used to normalize all the distributions to the same detector efficiency.

The smallest depth at which a radial distribution curve was measured was with the probe plate in the front position in the stack. In order to check the effect of the azimuthal asymmetry of the incident beam, a

radial distribution curve was also measured with the probe rotated and positioned horizontally at this depth and at a depth approximately 1 radiation length deeper. The effects due to the asymmetry were small and significant mainly in the first position. The logarithmic average of the two front-plate distributions was used in the final analysis of the data.

Any energetic electrons or photons striking the target, other than the beam of 900-MeV electrons, would deposit energy with a distribution different from that of the primary beam and hence would distort the measured shower development. The beam passes through a refocusing magnet after the energy-defining magnet and collimators. While this should remove most of the background radiation, some background radiation is produced by energy-degraded electrons which scatter from the walls of the beam-transport vacuum chamber. Attempts were made to eliminate this background by placing lead collimators, more than 10 cm thick and varying in hole diameter from 0.3 to 1.3 cm, after the refocusing magnet. Radial distribution curves, measured with the probe plate in the front of the stack, indicated that the amount of radiation reaching large radii was increased rather than decreased by the addition of collimators. This increase was found to be as much as a factor of 2 for the 1.3-cm-diam collimator. For this reason, collimators which defined both the vertical and the horizontal extents of the beam were used both before and after the energy-defining magnet, but no collimators were used after the refocusing magnet.

D. Data Reduction

The depth at which each radial distribution curve was measured was determined by measuring the amount of material in front of the probe plate and adding to that the effective depth due to the detector and the probe plate. The effective depth was taken to be the weighted average amount of detector material in front of the center of each detector, converted to radiation lengths, and added to the weighted average of the amount of material in the probe plate in front of the detector. This leaves a maximum uncertainty in the depth of the radial distribution curves of one half-width of the remainder of the probe well, which is 0.32 cm for the two smallest crystals. Calculations are being undertaken[13] to estimate this and other effects due to the probe well.

The data from each radial distribution curve were processed by an IBM 7090 computer. The ratio of the probe to the monitor signal was formed at each radial position, and the background was subtracted. The center of the distribution (or shower axis) was found by a least-squares procedure which was used to fit the logarithm of the ratio of the data points taken about the center to a parabola. The product of the ratio times the corresponding distance from the beam axis was computed to form the "ring distribution" (the amount of energy deposited in a thin ring). The ring distribution was then integrated over radius in 1-radiation-length segments from zero to the radius where the last experimental point was taken. Since the logarithm of the ring distribution was observed to decrease linearly as a function of radius (as previously observed by Kantz[7]), an extrapolation to infinite radius was used to calculate the remaining energy deposited at each depth. The transition curve was obtained by summing the integrals to find the total amount of energy deposited at each depth. In a similar manner, the results of the first integration were analyzed for fixed radius as a function of depth. The fraction of the incident energy deposited in each cylindrical ring, 1 radiation length in thickness and 1 radiation length in length, was found for the entire volume of the target in which shower data were measured. The amount escaping both radially and longitudinally was found by extrapolation. Representative radial distribution curves are shown in Fig. 3.

[13] D. Hubbard (private communication).

III. EXPERIMENTAL UNCERTAINTIES

The experimental limitations on the accuracy and resolution obtained in this experiment are discussed in Sec. II. Each point on the radial distribution curves was measured to an accuracy of better than $\pm 3\%$, the radial position to a resolution of ± 0.025 cm, and the depth of the probe plate to an accuracy of ± 0.08 cm. Additional sources of uncertainty in the experimental results are due to the possibility of temperature and fatigue effects on the photomultiplier tube, radiation damage to the CsI(Tl) crystal, and instabilities in the incident beam. To estimate the size of these effects, selected measurements were repeated, after an elapsed time of several days, and were found to reproduce to within an accuracy of better than 10%. The accuracy to which these data reproduce is indicative that other systematic effects associated with the experimental technique are the principal source of possible error in this experiment.

The most likely sources of systematic errors, not explicitly eliminated from this experiment, are associated with the determination of the effective depth of the measured points on the transition curve, the characteristics of the incident beam, and the energy-detection efficiency of the probe assembly. The maximum uncertainty in the depth of the radial distribution curves, due to the probe well size and the measurement of the depth of the probe plate is $+0.32$ cm, -0.08 cm. This is a very conservative estimate and all the results are consistent with an uncertainty in the depth of $+0.16$ cm, -0.08 cm. The probable errors are computed for this experiment using an uncertainty of $+0.16$ cm, -0.08 cm in the depth.

The asymmetry of the incident beam was determined as described in Sec. II. The measurements of the radial distribution curves with the probe positioned both vertically and horizontally are consistent with the image of the incident beam pictured in Fig. 2, which

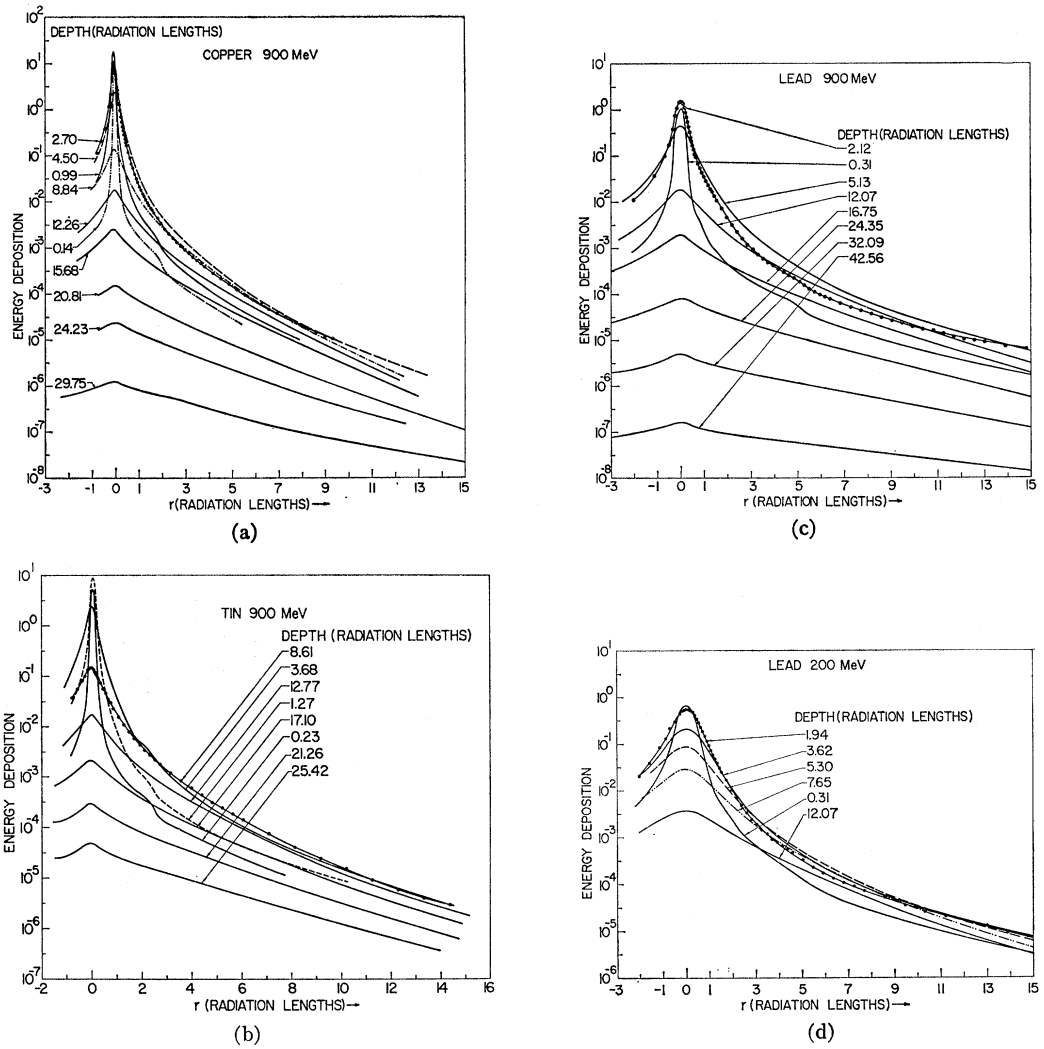

FIG. 3. Representative radial distribution curves are shown as visual fits to the data for each of the three target elements investigated with 900-MeV incident electrons and for lead with 200-MeV incident electrons. Each curve is determined by more than 100 individual measurements of the energy deposition as a function of the radial distance from beam axis for the more sharply peaked distributions, and between 50 and 100 measurements for the distributions at great depths in the shower. One curve is shown with the actual measured experimental points to illustrate the degree of scatter in the measured data. Irregularities in the radial distribution curves measured in front of shower maximum are due to background radiation striking the flanges in the beam transport system after the refocusing magnet. The effects of this background radiation on the measured distribution of energy deposition are discussed in Sec. III.

shows the beam to be taller (vertical direction) than it is broad (horizontal direction). The change in the total deposited energy determined from the vertically and horizontally measured distributions was on the order of or less than 10% beyond a depth 1.0 radiation length in tin and at all measured depths in lead. In the front plate, in tin, the difference between the vertically and horizontally measured distributions produced a difference in the total deposited energy of approximately 50%; for the front plate in copper, a difference of a factor of 2.0; and beyond a depth of 1.0 radiation length in copper, a difference of approximately 30%. The asymmetry effect is partially canceled by the use of the logarithmic average of the two front-plate distributions in the final analysis of the data. It is believed to affect the determination of the transition curve in front of shower maximum in lead by no more than 5%, in tin by no more than 10%, and in copper by no more than 20%.

The problem of the background radiation accompanying the incident beam is also discussed in Sec. II. Since the background radiation is poorly focused and collimated, some strikes the flanges on the exit window of the vacuum chamber and in the beam-monitoring ion chamber. In part, the effects of this on the radial distribution curves in front of shower maximum may be seen in Fig. 3. The radial distribution curves for 900-MeV incident electrons, measured with the probe plate in the front position in the stack, show irregularities at approximately 2.0 cm from beam center. This is the

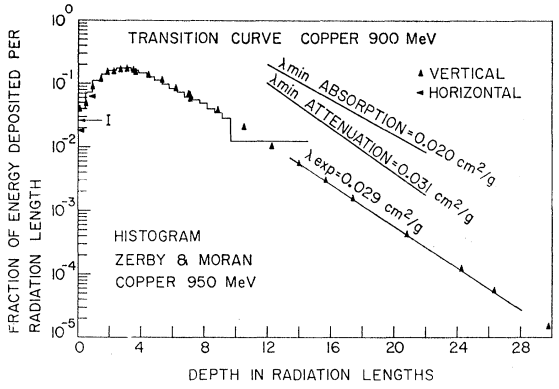

(a)

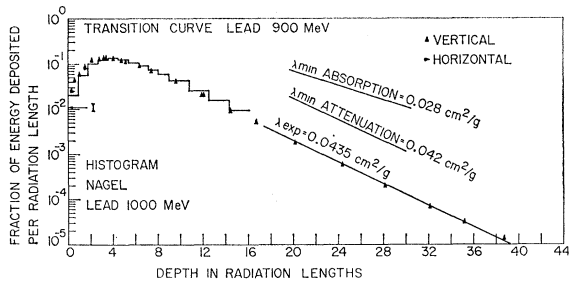

(c)

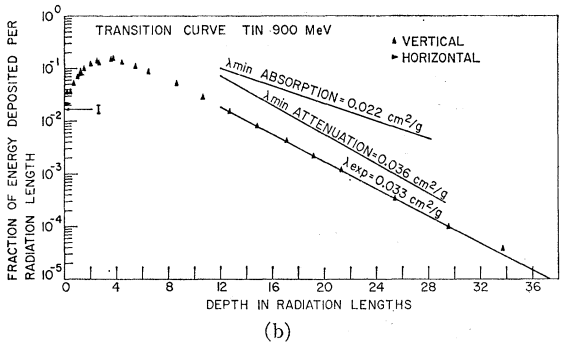

(b)

FIG. 4. The transition curves for 900-MeV electron-induced showers in copper, tin, and lead are shown as vertical and horizontal triangles representing deposited energy measured with the probe positioned vertically and horizontally, respectively. Each of these curves is normalized to unit area, so that the ordinate is the fraction of the incident energy deposited per radiation length while the abcissa is the depth of the measured energy deposition in radiation lengths. The arrows labeled "I" indicate the values calculated by Sternheimer for the fraction of the incident energy lost per radiation length through ionization by 900-MeV electrons. The quantity λ_{expt} for each transition curve is determined by a least-squares fit of the data. The lines drawn with λ_{min} absorption and λ_{min} attenuation are shown just to illustrate the slopes associated with these coefficients. The histogram from the calculations of Zerby and Moran for 950-MeV electron-induced showers in copper is normalized to unit area and shown with the copper transition curve from this experiment. The histogram from the calculations of Nagel for 1000-MeV electron-induced showers in lead is also normalized to unit area and shown with the lead transition curve from this experiment.

radius of the smallest constriction in the beam transport system after the refocusing magnet. It is estimated that this background has an insignificant effect on the measured energy distribution because at this radius, the amount of energy deposited is four orders of magnitude less than the peak value. For each target material the integrated amount of energy deposited outside this radius lies between 2 and 4% of the fraction deposited at that depth. This is small and in good agreement with the predictions of the Monte-Carlo calculations of Nagel.[5]

During this experiment, the beam transport system was optimized for the study of 900-MeV electron-induced showers. At 200 MeV, the poorer collimation and focus of the electron beam could account for higher levels of low-energy background radiation at the first few measured depths. No significant asymmetry of the incident beam was found even at the smallest measured depth.

To be a measure of the spatial distribution of energy deposition in the shower, the signal from the probe must be linearly proportional to the energy stopped in the CsI(Tl) detector, which in turn must have a stopping power proportional to that of the target material over the entire range of energies of both the electrons and the photons present throughout the shower. A study carried out at Stanford[14] obtained precise measurement of the efficiencies of seven different scintillator–photomultiplier-tube combinations as a function of the energy of the incident γ ray stopped in the scintillator detector. Deviations in the efficiency on the order of $\pm 20\%$ were found for incident γ-ray energies between 600 and 4 keV for a CsI(Tl) scintillator in combination with an EMI 9514S photomultiplier tube. Efficiency measurements of a NaI(Tl) scintillator in combination with both an Amperex XP1010 and an EMI 9514S photomultiplier tube indicate that the changing efficiency may be due to a spectral shift of the light output of the scintillator and the frequency response of the photocathode surface. A change in the efficiency of $\pm 20\%$ over a small energy range would not greatly affect the results of this experiment, although the properties of the detectors warrant further study.

Matching the stopping power of the detector to that of the target material is a problem considered by Kantz and Hofstadter.[8] They showed that the stopping power of CsBr(Tl) is similar to that of copper over a range of energies from 0.8 to 100 MeV for both electrons and photons. In the present experiment, the atomic numbers of the detector, $Z=55$ for cesium and $Z=53$ for iodine, are very nearly the same as the atomic number of tin, $Z=50$; so the stopping power of the detector is approximately the same as that of tin. Kantz[7] obtained two radial distribution curves measured in lead, one with a CsBr(Tl) detector and the other with a $CaWO_4$ detector. Negligible differences were noted between the responses of the two detectors, although a superior match to lead was given by $CaWO_4$ because of the high

[14] D. W. Aitken, B. L. Beron, G. Yenicay, and H. R. Zulliger, IEEE Trans. Nucl. Sci. **NS14**, 468 (1966).

TABLE II. Energy lost by ionization in MeV cm^2 g^{-1}.

Target element	Sternheimer[a] 900-MeV incident electrons	This experiment 900-MeV incident electrons	Nelson *et al.*[b] 1000-MeV incident electrons	Sternheimer[a] 200-MeV incident electrons	Kantz[c] 185-MeV incident electrons	Murata[d] 200-MeV incident electrons
Copper	1.83	1.6+0.2, −0.3	0.5	1.72	1.0	...
Tin	1.70	2.0+0.3, −0.4	...	1.60	1.1	...
Lead	1.56	2.4+0.5, −1.0	1.9	1.48	1.1	1.4

[a] R. M. Sternheimer, Phys. Rev **88**, 851 (1952); **91**, 256 (1953); **103**, 511 (1956).

[b] These values were not calculated by W. R. Nelson *et al.*, but were taken from their transition curves (Figs. 10 and 11) [Phys. Rev. **149**, 201 (1966)].

[c] A. Kantz, Ph.D. thesis, Stanford University, 1954 (unpublished), Stanford University High Energy Physics Laboratory Report No. 17; 1954 (unpublished).

[d] Y. Murata, J. Phys. Soc. Japan **20**, 209 (1965).

atomic number, 74, of the tungsten. This would indicate that the match between CsI(Tl) and lead should not cause any serious distortions in the measurement of energy deposition in that target material. Although the atomic number of copper is slightly closer to the average atomic number of CsBr(Tl) than to that of CsI(Tl), the two detectors are so similar that the results should be equally valid.

IV. RESULTS

A. Energy Balance

The transition curves for electron-induced showers at 900 MeV in copper, tin, and lead are shown in Fig. 4. The triangles indicate the experimental points obtained in this investigation, normalized so that the area under each curve is unity. At zero depth, the electrons in the monoenergetic beam lose energy primarily by bremsstrahlung and by ionization of the target medium. The energy lost to bremsstrahlung is transported into the shower medium, but the energy lost by ionization is rapidly deposited in the target material. It was pointed out by Kantz and Hofstadter,[7,8] that the values of the ordinate at zero depth, which correspond to energy deposition, should also correspond to that fraction of the incident energy lost per unit depth (dE/dx) by ionization of the target material. Agreement between the experimentally determined value of dE/dx at zero depth and the theoretical value of dE/dx due to ionization loss is called energy balance. This ionization loss has been calculated by Sternheimer[15] (including both relativistic and density effects) as a function of the atomic number of the target material and the energy of the incident electron. The results computed from Sternheimer's equation are indicated by arrows labeled I in Fig. 4 and are given in Table II along with the experimental values of Nelson *et al.*,[10] Kantz,[7] and Murata.[11] The experimental values for this experiment were determined by a least-squares fit of the data taken before shower maximum to the form $\exp(A+Bt+Ct^2)$, where A, B, and C are the fitting parameters, and t is the depth in the shower. The agreement is satisfactory and within the estimated experimental uncertainties.

[15] R. M. Sternheimer, Phys. Rev. **88**, 851 (1952); **91**, 256 (1953); **103**, 511 (1956); **145**, 247 (1966).

In this experiment, the incident beam of electrons was steered before the measurement of each radial distribution curve so that the detector passed through the beam axis to within an accuracy of 0.025 cm. In the experiment of Nelson *et al.*,[10] however, the beam center was determined optically before the beam intensity was reduced to the level at which the detectors for the radial distribution curves were exposed. A mis-steering of the incident beam by 0.1 cm in the experiment of Nelson *et al.* would account for the lack of energy balance, by nearly a factor of 4, for the transition curve from 1000-MeV electrons incident on copper. The value of dE/dx obtained from the results of Nelson *et al.* for 1000-MeV electrons incident on lead is in good agreement with the theoretical value of the ionization loss calculated by Sternheimer, although the uncertainties in the steering of the incident beam are the same as in the case of copper.

The values of dE/dx obtained by Kantz are all lower than the values calculated by Sternheimer. In calculating the effective depth of the detector, Kantz did not include the number of radiation lengths due to the detector itself. Had he included this contribution to the depth, his values of dE/dx would have been even lower. The measured horizontal and vertical radial distribution curves indicate that asymmetry of the incident beam was not a problem. The height and the diameter of the CsBr(Tl) detector used by Kantz were each four times larger than those of the smallest crystal used in this experiment, so it is probable that poor resolution tended to depress the early part of the transition curve. Also, it is probable that background radiation produced in the collimators distorted the measured development of the showers.

No estimate is given by Murata on the experimental accuracy of his determination of energy balance.

B. Energy-Absorption Coefficients

Another characteristic feature of shower development is the portion of the transition curve past shower maximum, which decreases exponentially with depth. This portion of the transition curve is observed to be of the functional form $Ae^{-\lambda t}$, where A is a constant, λ is the fractional rate of decrease of the tail of the transition curve, and t is the depth in the shower. In previous

TABLE III. Comparison of experimentally determined coefficients with γ-ray absorption and attenuation coefficients.

Target element	λ_{min}[a] absorption ($cm^2\ g^{-1}$)	λ_{min}[a] attenuation ($cm^2\ g^{-1}$)	λ_{expt} this experiment ($cm^2\ g^{-1}$)	λ_{expt}[b] Nelson *et al.* ($cm^2\ g^{-1}$)	λ_{expt}[c] Kantz ($cm^2\ g^{-1}$)
Copper	0.020	0.031	0.029	0.024	0.0292
Tin	0.022	0.036	0.033	...	0.0344
Lead	0.028	0.041	0.0435	0.045	0.0408

[a] W. S. Snyder and J. L. Powell, Oak Ridge National Laboratory Report No. ORNL 421, 1950 (unpublished); also quoted in O. I. Leipunskii, B. V. Novozhilov, and V. N. Sakharov, *The Propagation of Gamma Quanta in Matter*, translated by Prasenjit Basu, 1st English edition edited by K. T, Spinney, J. Butler, and J. B. Sykes. (Pergamon Press, Oxford, England. 1965.)

[b] W. R. Nelson, T. M. Jenkins, R. C. McCall, and J. K. Cobb, Phys. Rev. **149**, 201 (1966).

[c] A. Kantz, Ph.D. thesis, Stanford University, 1954 (unpublished); Stanford University High Energy Physics Laboratory Report No. 17, 1954 (unpublished).

work, it has been assumed that the measured value of λ, λ_{expt}, should correspond to the energy-absorption coefficient for minimum-absorption γ rays. Even though it is energy deposition that is being measured, the experimental results have not agreed with this simple minimum-absorption model. The minimum-absorption γ rays deposit a significant fraction of their energy by the Compton process, whereby they lose only part of their energy to electrons. The remainder propagates into the shower medium in the form of lower-energy γ rays, which are absorbed at a higher rate than the minimum rate. One difficulty with the minimum-absorption model is that it fails to account for the rate at which energy is lost by these lower-energy γ rays. A more accurate estimate would be an average of the absorption coefficient, which depends on the energy of the γ ray, weighted by the energy spectrum of the particles present. Calculations have been performed for copper and lead absorbers, assuming both flat and bremsstrahlung spectra, and each with several different upper limits on the γ-ray energy. The results of this averaging technique are strongly dependent on the value of the highest γ-ray energy included in the spectrum. The choice of the cutoff energy is arbitrary, and for each case (except for that of a bremsstrahlung spectrum in lead), agreement with the experimental results can be obtained by a suitable choice of the cutoff energy between 15 and 20 MeV. For the bremsstrahlung spectrum in lead, the best choice of cutoff energy gives a value that is 10% higher than the measured value. It is clear from these results that λ is dependent on the spectrum of γ rays present in the shower.

Another approach has been suggested,[16] analogous to the parent-daughter decay rates in radioactive decay schemes.[17] Gamma rays, whose energies lie near the minimum of the attenuation curve, are the most penetrating of the principal energy-transporting components of the shower. The exponential decrease of the transition curve suggests that the spectrum of particles may have reached a type of "secular equilibrium," which would consist primarily of minimum-attenuation γ rays and the products of their interactions. These products are of lower energy and are attenuated more rapidly than the minimum-attenuation γ rays. Under these assumptions the transition curve should decrease at a composite rate which is slightly less than the minimum attenuation coefficient for γ rays. In Fig. 4 lines corresponding to both the minimum-absorption and the minimum-attenuation coefficients are shown for the three target elements. Good agreement with the minimum-attenuation coefficient is obtained in each case. The tabulated results are given in Table III along with the values obtained by Nelson *et al.* and by Kantz. Murata does not present sufficient data to determine this coefficient.

C. Transition Curves

The histogram from the Monte-Carlo calculation by Zerby and Moran[18] for 950-MeV electron-induced showers in copper is presented with the data for copper, Fig. 4(a). The histogram is also normalized to unit area for comparison with the data. The calculation is limited by a cutoff energy of 2 MeV for both electrons and photons. Curves shown by Zerby and Moran[4] indicate that the principal effects of lowering the cutoff energy would be to move the maximum in the shower curve, called shower maximum, to a greater depth by approximately 0.1 radiation length and to reduce the relative height of shower maximum on the order of 10%. These changes would tend to improve the agreement, although they are less than the experimental uncertainties associated with these measurements. The general characteristics of the transition curve are only a slowly varying function of the energy of the incident electron, so a comparison of this experiment at 900 MeV and of the experiment of Nelson *et al.* at 1000 MeV with the Monte-Carlo calculation at 950 MeV is reasonably justified. The data are in good agreement with these results and confirm the calculations of Zerby and Moran on the development of the shower in front of shower maximum, in contrast with the results of Nelson *et al.* (See Fig. 10, Ref. 10.)

The transition curve for tin is shown in Fig. 4(b).

The histogram from the Monte-Carlo calculations by Nagel[5] for 1000-MeV, electron-induced showers in lead

[16] D. Quinn (private communication).

[17] R. Evans, *The Atomic Nucleus* (McGraw-Hill Book Company, Inc., New York, 1955).

[18] C. D. Zerby and H. S. Moran (private communication).

is presented with the data for lead, Fig. 4(c). The histogram is also normalized to unit area for comparison with the data. In this more recent calculation, the cutoff energy for electrons is 1.5 MeV and that for photons is 0.25 MeV, which should be adequate for a good description of the transition curve. The data from this experiment are in better agreement with the shape of the transition curve predicted by Nagel, than the data reported by Nelson *et al.* (see Fig. 11, Ref. 10). The systematic disagreement of the data of the present experiment with the calculation of Nagel would disappear if each experimental point were assigned a depth 0.3 radiation lengths deeper in the shower. This corresponds to a measured distance of 0.17 cm, which is of the order of the possible systematic error in the depth which was discussed in Sec. III.

Although the emphasis in this experiment was on showers induced by 900-MeV electrons, differences between the results of Kantz and Hofstadter and the more recent results of Murata made it of interest to investigate the shower development from 200-MeV incident electrons as well. The data for 200-MeV electrons incident on lead were measured with the same normalization as the 900-MeV data in lead, so that the areas under their transition curves should be in the ratio of 900 to 200. The ratio obtained from the experimental results is 4.3. This is a favorable indication of the reliability of the techniques employed in this experiment. The two transition curves are shown in Fig. 5, normalized so that the area under the 900-MeV curve equals 900 MeV.

While the uncertainty in the measured depths of the radial distribution curves is the same as at 900 MeV, the asymmetry of the electron beam at 200 MeV is negligible. These experimental uncertainties in the 200-MeV

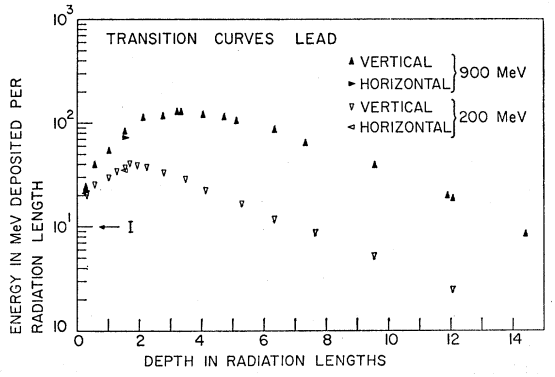

FIG. 5. The transition curves for 900- and 200-MeV electron-induced showers in lead are shown as vertical and horizontal triangles representing deposited energy measured with the probe in vertical and horizontal positions, respectively. The normalization of both curves is the same and was determined by setting the area under the 900-MeV transition curve equal to 900 MeV, so that the ordinate is the energy in MeV deposited per radiation length while the abcissa is the depth in radiation lengths. The arrow labeled "I" indicates the value calculated by Sternheimer for the energy lost per radiation length through ionization by 900-MeV electrons. The energy lost per radiation length by 200-MeV electrons differs by less than the width of the arrow.

transition curve in lead are not sufficient to explain the failure of the curve to extrapolate to the predicted value of dE/dx at zero depth. It is possible that the first few measured depths are distorted by the higher levels of low-energy background discussed in Sec. II. However, the agreement between the total areas under the lead transition curves at 900 and at 200 MeV indicates that the background at 200 MeV is not more than 5% of the total energy in the 200-MeV shower. For this small amount of possible background radiation to explain the failure of the 200-MeV curve to energy balance, it must all be deposited in the first few measured depths and not significantly distort the shower at or beyond shower maximum. Kantz and Hofstadter find shower maximum at 2.3 radiation lengths; Murata at 1.9 radiation lengths; and Zerby and Moran[4] predict it to be between 1.8 and 2.0 radiation lengths. (All results are corrected to agree with the value of a radiation length $\chi_0=6.5$ g cm^{-2}.) In this experiment, shower maximum is found at 1.8 ± 0.3 radiation lengths, which is in better agreement with the result of Murata and the prediction of Zerby and Moran, but not outside reasonable estimates of experimental uncertainty in the experiment of Kantz and Hofstadter.

D. Radial Escape Curves

It has been suggested by Nelson *et al.*[10] that the fraction of the incident energy escaping from an infinitely long cylinder, when plotted versus the radius divided by the Molière length,[19] might form a universal curve. These plots, called radial escape curves, are shown in Fig. 6. The data of Nelson *et al.* are seen to be in good agreement with the predictions of Nagel [Fig. 6(a)] and the data of Murata give moderate agreement [Fig. 6(b)]. For copper, tin, and lead, the results of this experiment [Fig. 6(a)] and the experiment of Kantz and Hofstadter [Fig. 6(b)] yield curves which fall farther away from the Nagel prediction the lower the atomic number of the target material. This is the behavior that one might expect if annihilation radiation, which is neglected in the Monte-Carlo calculations of Nagel, were an important mechanism in the transport of energy away from the shower axis. Kantz and Hofstadter have previously suggested that annihilation radiation could be a significant process in shower development. The annihilation γ radiation would penetrate to larger radii, the lower the atomic number of the target material. For minimum-attenuation γ rays in lead,

$$r_a/r_M=1.31,$$

and in copper

$$r_a/r_M=2.25,$$

where r_a is defined to be the distance in which $1-1/e$ of the γ rays are attenuated, and r_M is the Molière

[19] If the radius is expressed in g cm^{-2}, then the Molière length r_M is given by $\chi_0 E_s/\epsilon_0$, where χ_0 is the value of 1.0 radiation length in the material, expressed in g cm^{-2}; E_s is 21.2 MeV; and ϵ_0 is the critical energy of the material expressed in MeV.

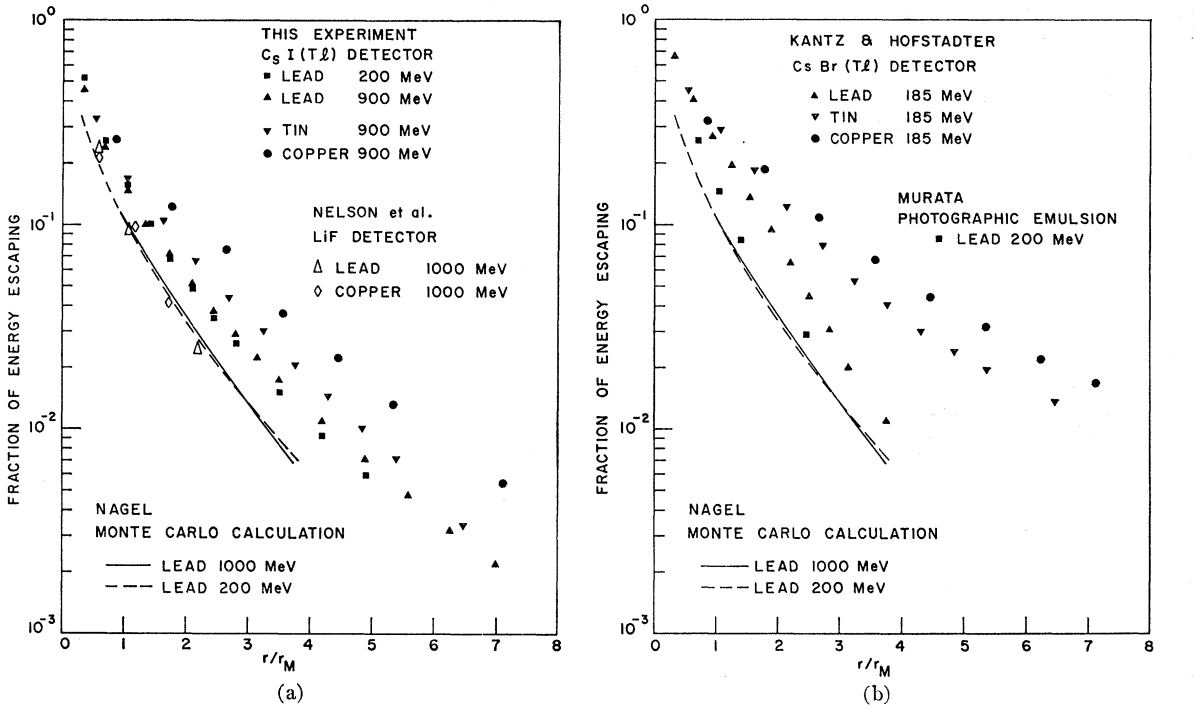

FIG. 6. The fraction of the incident energy escaping from an infinitely long cylinder of radius r is shown as a function of r/r_M, where r_M is the Molière length. The data from several different experiments are compared with the predictions of the Monte Carlo calculations by Nagel. The values for the radiation length and the critical energy, used in calculating the Molière length for copper, tin, and lead are given in Table I. The uncertainties associated with these radial escape curves are discussed in the Sec. IV.

length. The values of r_a/r_M may be thought of as penetration lengths for minimum-attenuation γ rays, expressed in the Molière units of the respective materials. Because of the dependence of the penetration length on the atomic number of the absorbing material, any given fraction of the incident energy transported by minimum-attenuation γ rays would be expected to escape at a larger radius (expressed in Molière units) the lower the atomic number of the target material. Possibly these effects were not observed by Nelson *et al.* and Murata, because their detectors were of low atomic number and relatively insensitive to all γ radiation.

The uncertainties associated with these radial escape curves are due to possible systematic effects in the experimental measurements and uncertainties in the exact values of the critical energies and of the radiation lengths. The experimental uncertainties in the present experiment are approximately twice the size of the data points for values of the energy escaping greater than 2% of the incident energy. For values of the energy escaping less than 2% of the incident energy, the uncertainties are approximately 0.5% of the incident energy. Uncertainties in the constants used to calculate the values of the Molière lengths may be as large as 20%, but would tend to shift all the curves systematically and would not change the relative values significantly.

However, the results of Kantz and Hofstadter for showers in carbon and aluminum, probed with an anthracene $[C_6H_4:(CH)_2:C_6H_4]$ detector, show a reverse trend. Their aluminum data fall farther from the curve predicted by Nagel than do their carbon data. Since there are uncertainties in the choice of the exact values of the critical energies and of the radiation lengths, as well as possible uncertainties in the experimental measurements, the significance of these data is not known. A knowledge of the spectrum of photons as a function of depth and radius in the shower would assist in clarifying these results.

V. SUMMARY AND CONCLUSIONS

Electromagnetic cascade showers induced by 900-MeV electrons have been studied in copper, tin, and lead targets. In addition, data for showers induced by 200-MeV electrons in lead were obtained. Radial distribution curves of energy deposition have been measured with a CsI(Tl) detector placed at various positions in a small hole in the otherwise solid target. The transition curves were obtained by integrating the results of the radial distribution curves measured at different depths in the target material. Radial escape curves for each of the target elements have also been determined.

Energy deposition in 900-MeV electron-induced showers is such a rapidly varying function of depth in front of shower maximum that there are large uncertainties in the experimental determinations of the energy

deposited at zero depth. The agreement between the measured values of energy deposition at zero depth obtained in this experiment and the theoretically predicted values of energy loss by ionization is well within these experimental uncertainties.

The measured values of the fractional rates of decrease of the tails of the transition curves obtained in this experiment for copper, tin, and lead are in good agreement with the values obtained with 185-MeV incident electrons given by Kantz[7] and are in good agreement with the corresponding minimum attenuation coefficients for each of the three materials.

The transition curves for 900-MeV electron-induced showers in copper and lead, obtained in the present experiment, confirm the results for the longitudinal distributions of energy deposition predicted by the Monte-Carlo calculations of Zerby and Moran[18] and Nagel,[5] respectively.

The radial escape curves obtained in this experiment for copper, tin, and lead deviate from the curves calculated by Nagel and the measured points of Nelson *et al.*[10] The deviations are larger the smaller the atomic number of the target material. The results obtained by Kantz and Hofstadter[8] for 185-MeV electron-induced showers in copper, tin, and lead showed similar deviations. While the radial escape curves measured in the present experiment show a dependence on the atomic number of the target material, radial escape curves measured with the same target (lead) but with two different incident-electron energies, 200- and 900 MeV, are the same to within the uncertainties associated with this experiment.

A possible explanation for the behavior of the radial escape curves is that energy is transported laterally by annihilation radiation, which has been neglected in the Monte-Carlo calculations. The annihilation γ rays can penetrate to greater distances the lower the atomic number of the target material. The detectors used by Nelson *et al.* and Murata[11] are of low atomic number and relatively insensitive to all γ radiation. Presently available information on the lateral transport of energy in cascade showers is not sufficient to fully explain these results. Nevertheless, calculations of the importance of annihilation radiation as an energy-transporting mechanism could supplement the predictions of the Monte-Carlo calculations on the lateral distribution of energy.

Another line of endeavor which might help to clarify the interpretation of these results would be an investigation of the energy spectrum of photons as a function of lateral and longitudinal position in the shower. This could be obtained by pulse-height analysis of pulses in a large probe crystal. It is anticipated that elements of the target and detector assembly used in the present experiment could be employed for this purpose. This investigation might help to determine the importance of annihilation radiation in the propagation of energy at large angles to the shower axis.

As this experiment progressed, techniques were improved for using the experimental IBM data-acquisition system[20] to obtain and analyze shower data more rapidly. It should be possible to measure an entire radial distribution curve without any manual interruption from the experimenter. With this closed-loop system, additional material, such as the low-atomic-number elements, could be investigated with increased efficiency. Medical interest in the deposition of energy by showers in human tissue makes water an interesting target. Aluminum is also an interesting target because of its similarity to concrete which is used as a shielding material.

Better understanding of the spectral response of detectors, the spatial distribution of energy spectra in the shower, and the behavior of showers as a function of the atomic number of the target material, will make the results of the Monte-Carlo calculations more meaningful and will indicate areas for further investigation.

ACKNOWLEDGMENTS

The author is grateful to all those who assisted in the performance of this experiment: to Professor Robert Hofstadter for suggesting this experiment and making his advice and comments available; to Professor Robert Mozley for providing equipment and for suggestions during the development of this experiment; to Dr. Hall Crannell and Professor Mason Yearian for helpful suggestions, for assistance with the data acquisition, and for reading this manuscript; to Dr. Andrew Browman and Professor David Ritson for stimulating conversations and comments; to Walter R. Nelson for making references available and for interesting suggestions; to Robert Parks for the design of the target and detector assembly; to Marinus Ryneveld for the design of the beam monitor and assistance in programming the data acquisition system; to Frank Bloch and Katsuchika Goto for assistance with the data acquisition and reduction; and to all the members of the laboratory staff who helped construct and set up the experimental apparatus, provide the electron beam, record and reduce the data, and prepare this manuscript. Their personal interest in the progress of this work is sincerely appreciated.

[20] M. R. Yearian, C. J. Crannell, H. Crannell, D. C. Smith, P. J. Friedl, C. Sederholm, and W. Dye, IEEE Trans. Nucl. Sci. **NS14**, 608 (1966).